Int. J. Heat Mass Transfer. Vol. 15, pp. 2077–2089. Pergamon Press 1972. Printed in Great Britain

FORCED CONVECTION DROPLET EVAPORATION WITH FINITE VAPORIZATION KINETICS AND LIQUID HEAT TRANSFER

WARREN C. STRAHLE

School of Aerospace Engineering, Georgia Institute of Technology, Atlanta, Georgia, U.S.A.

(*Received* 16 *September* 1970 *and in revised form* 15 *November* 1971)

Abstract—Stagnation point calculations, including the effects of liquid phase heat transfer and finite rate evaporation kinetics, are presented for the case of a high Reynolds number flow over a vaporizing droplet. A correlation is developed to compute the entire droplet vaporization rate from the stagnation point results. Numerical emphasis is placed on high temperature, rapid vaporization processes such as occur in flight vehicle engines, and sufficient calculations are presented to allow estimates for any given case to be made.

NOMENCLATURE

$a_1, a_2, a_3, b_1, b_2, b_3, c_1, c_2$, constants in the approximating functions for f, g and Y_F;
a, nose radius of curvature;
B, c_pT_δ/L;
c_p, specific heat at constant pressure for the gas phase;
c_L, liquid phase specific heat;
f, stream function;
f_0, stream function at interface;
g, temperature, T/T_δ;
L, latent heat of vaporization;
$\dot{m}$, total droplet vaporization rate;
$\bar{m}$, vaporization rate per unit surface area;
m, $(\alpha/2)[p/\pi(\mathrm{d}u/\mathrm{d}x)_0\mu_0]^{\frac{1}{2}}$;
p, total pressure;
p_v, liquid vapor pressure at interface temperature;
Re, Reynolds number $(\rho_\infty u_\infty a/\mu_\infty)$;
T, temperature;
T_{L_0}, initial liquid temperature;
u, velocity parallel to surface;
u_∞, free stream oncoming velocity;
v, velocity normal to surface;
x, distance parallel to surface;
Y, ratio of p_v to p;
Y_F, fuel mass fraction;
Y_{F_0}, ratio p_v/p at T_{L_0};
Y_s, $Y_F(0)$;
y, distance normal to surface;
α, evaporation coefficient;
α_L, liquid phase thermal diffusivity, λ_L/ρ_Lc_L;
ε_v, $L/c_pT_{L_0}$;
λ, thermal conductivity;
μ, viscosity;
η, transformed normal distance;
ρ, density.

Subscripts

b, interface;
L, liquid;
L_0, liquid phase before heat up has occurred;
δ, edge of boundary layer;
∞, free stream.

INTRODUCTION

IT IS often necessary to obtain estimates of the time required to vaporize liquids injected into a high temperature gas phase environment. For example, highly useful calculations have been presented for rocket propellants by Priem and Heidmann [1]. Quite often, as in [1], the

majority of a droplet's lifetime and certainly the portion of the lifetime during which the greatest vaporization rate occurs is spent in a high Reynolds number condition with respect to the gas phase environment; say, $Re > 10$. Such a condition suggests a laminar boundary layer existence over the leading edge of a droplet. Since boundary layer thicknesses, and consequently the inverse of heat and mass transport rates, do not increase by over a factor of two over the leading eige of a body [2] and separation phenomena over the trailing edge substantially reduce transport rates, it is reasonable to assume that the stagnation point behavior is dominant in determining the overall vaporization rate of a droplet. Consequently, attention will be paid in this paper to the stagnation point region, as far as detailed calculations are concerned; the relation to the entire droplet vaporization rate will then be deduced.

The need for a new approach to the calculation of stagnation point evaporation rates comes from the mounting evidence that a thermal profile exists in the liquid state as opposed to a uniform temperature distribution, which may be time varying, eventually approaching the wet-bulb condition. Recent transient calculations [3] have shown that the thermal heating wave penetrating the liquid phase cannot be expected to reach the droplet center in a high Reynolds number flow. There is also support for the view that even in a low Reynolds number flow a thermal wave assumption is preferable to a vaporization (volatile fuel in the given environment) and especially if the low Reynolds number portion of the lifetime is short [4]. The existence of a thermal wave changes the energy balance at the liquid–gas interface over that obtained by assuming the liquid heats in bulk or does not heat at all (the wet-bulb condition). Consequently the vaporization rate will change as compared with a different assumption concerning the liquid phase behavior. An assumption of bulk heating would be reasonable if there were sufficiently rapid internal circulation in the liquid. However, simple order of magnitude considerations concerning viscous shear and surface tension induced flows suggest that the liquid is essentially static internally and that the thermal wave assumption is preferable to a uniform temperature assumption.

The physical effects of a nonadiabatic interface are known [5]; clearly, the vaporization rate is reduced if the liquid is a heat sink. However, proper calculations have never appeared so that actual estimates of droplet vaporization rates for a wide variety of cases can be easily made. The present paper attempts to provide these results.

It is also a common assumption, as in [1], to assume that the liquid–gas interface is in equilibrium so that the partial pressure of the droplet vapor at the interface corresponds to its equilibrium vapor pressure at the interface temperature. At sufficiently high pressures and with large enough droplets this is a reasonable assumption, but there are regimes of practical interest, primarily in high altitude flight and with fuels possessing restricted molecular rotation in the liquid state, where the validity of an equilibrium interface disappears [6]. Again, the physics of a finite rate process are understood; obviously the vaporization rate decreases for a finite rate process as opposed to an infinite rate equilibrium process. However, there have never appeared computations for the droplet vaporization process with sufficient generality to estimate the magnitude of the effect for a given case. The present paper presents sufficient numerical results concerning the finite rate effect to be useful in calculation of vaporization rates. Numerical emphasis in all results below is given to high temperature vaporization processes such as those found in liquid propellant rockets, turbojets, ramjets, supersonic combustors, and external burning.

ANALYSIS

Stagnation point

Consider the axially symmetric stagnation point configuration of Fig. 1. Usual simplifying

assumptions are made here which restrict the general accuracy in application, although in practice more severe errors are usually introduced by the choice of transport data. The

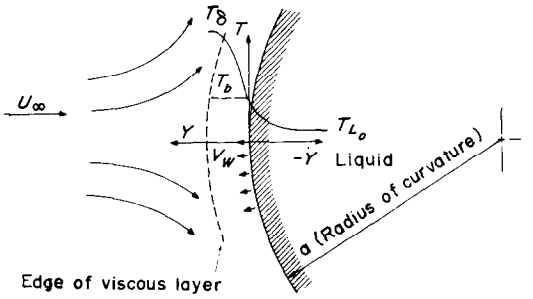

FIG. 1. Stagnation point schematic.

assumptions are a boundary-layer flow, perfect gas constituents, Prandtl and Lewis numbers of unity, heat transfer by conduction only, gas viscosity proportional to temperature, mass transfer by a concentration gradient only, and a constant specific heat regardless of local mixture ratio. Of course, continuum flow is assumed. The well known stagnation point equations for the gas phase then become

$$\begin{aligned} f''' + ff'' + \tfrac{1}{2}[g - f'] &= 0 \\ g'' + fg' &= 0 \\ Y_F'' + fY_F' &= 0 . \end{aligned} \tag{1}$$

The independent variable η is defined by

$$\eta = \left[2\rho_b \left(\frac{\mathrm{d}u}{\mathrm{d}x}\right)_0 \Big/ \mu_b\right]^{\frac{1}{2}} \int_0^y (\rho/\rho_b)\,\mathrm{d}y'$$

and f is the stream function so defined that

$$f = u/u_\delta .$$

The liquid phase is treated as a semi-infinite mass; this is valid if the penetration of the thermal wave is much less than the nose radius of curvature. For a high Reynolds number exterior flow this has been shown in [3] to be the case; for a low or zero Reynolds number flow this is not in general true except for extremely volatile fuels or during the transient portion of the development of the heating wave. Consequently, the validity of the present treatment rests upon the maintenance of a high Reynolds number flow over the majority of the droplet's lifetime. The liquid–gas interface is maintained at $y = 0$ by translating the liquid toward the origin at the instantaneous regression rate. This is allowable with no further consideration of wave motion in the liquid under an incompressibility assumption for the liquid phase. In the vicinity of the stagnation point, therefore, the heat balance is one of conduction balancing convection and the differential equation is

$$\alpha_L \frac{\mathrm{d}^2 g_L}{\mathrm{d}y^2} = v_L \frac{\mathrm{d}g_L}{\mathrm{d}y} . \tag{2}$$

The use of a steady state equation also requires that the liquid shape is not distorting in time. The justification for this assumption is presented below. The solution to equation (2) under the boundary conditions $g_L(0) = g_b$, $g_L(-\infty) = g_{L_0}$ is

$$(g - g_{L_0}) = (g_b - g_{L_0}) \exp\left[(v_L/\alpha_L)y\right] . \tag{3}$$

The heat transfer into the liquid is consequently

$$\lambda_L \left(\frac{\mathrm{d}g_L}{\mathrm{d}y}\right)_b = \left(g_b - g_{L0}\right) \frac{v_L}{\alpha_L} \lambda_L . \tag{4}$$

From equation (3) the condition, as assumed, for the thermal wave to be of a small thickness is that $\alpha_L/v_L \ll a$. Mass continuity requires $\rho_L v_L = \rho_b v_b$ and in a boundary layer flow v_b is $0[u_\infty/Re^{\frac{1}{2}}]$ so that $\alpha_L/v_L = \alpha_L\rho_L/\rho_b v_b = \lambda_L/\rho_b c_L v_b$ is $0[aRe^{-\frac{1}{2}}]$. Thus, the assumption is satisfied in a high Reynolds number flow. It should be realized that translation of the liquid toward the gas to maintain the interface at $y = 0$ is not sufficient to maintain the interface at a constant position, since the droplet size must decrease with time. Therefore, equation (2), which is a steady state equation, is generally incorrect. However, the comparison which is relevant in this case is a comparison of the droplet

lifetime with a characteristic heat transfer time in the liquid. The orders of magnitude of these times have been presented previously [7] for the case at hand of a thin thermal wave depth compared with the droplet radius. The order of magnitude of the droplet lifetime is $\rho_L a^2/\mu_\delta$ while the magnitude of the characteristic heat transfer time is $\rho_L \lambda_L a^2/\mu_\delta^2 c_L$. The ratio of the droplet lifetime to the heat transfer time is consequently of the order of $\mu_\delta c_L/\lambda_L$. This parameter is usually quite small ($< 10^{-1}$) for most situations. Therefore, there is insignificant droplet surface contraction in the characteristic time scale of the liquid heat transfer process.

From the definition of the stream function the vaporization rate is

$$\rho_L v_L = \rho_b v_b = -f_0 \left[2\rho_b \mu_b \left(\frac{du}{dx}\right)_0\right]^{\frac{1}{2}}. \tag{5}$$

Using equations (4) and (5) the energy balance at the interface becomes

$$g_b' = -f_0 \left[\frac{1}{B} + \frac{c_L}{c_p}\left(g_b - g_{L_0}\right)\right]. \tag{6}$$

For all numerical computations below $c_L = c_p$ is assumed, since c_L/c_p has been found to have little effect; a change in c_L/c_p produces a compensating change in $g_b - g_{L0}$. A direct comparison of the amount of heat going into the liquid to the heat going toward vaporization is provided by comparison of $(g_b - g_{L0})$ with $1/B$. It will be shown that the liquid heating rate can be substantial. A further condition at the interface is that of temperature continuity, $g(0) = g_b$, and at the edge of the gas phase viscous region $g(\infty) = 1$. The boundary conditions on the momentum equation of equations (1) are

$$f'(0) = 0 \qquad f'(\infty) = 1 \qquad f(0) = f_0. \tag{7}$$

The quantities f_0 and g_b cannot be specified, however, since they depend upon the mass transfer and interface kinetics processes. The conditions on Y_F are

$$\begin{aligned} &Y_F(0) = Y_s \quad Y_F(\infty) = 0 \\ &Y_F'(0) = f_0(1 - Y_s). \end{aligned} \tag{8}$$

A new unknown Y_s has been introduced but the last of equations (8) introduces a relation between f_0 and Y_s which expresses the mass diffusion rate at the interface. Equation (6) gives a relation between f_0 and g_b and only one variable is left undetermined, Y_s. The Knudsen–Langmuir formula derived from absolute rate theory is used here [6]

$$f_0 = \frac{\alpha}{2}\left[\frac{p}{\pi(du/dx)_0 \mu_\delta}\right]^{\frac{1}{2}} \left[\frac{Y_s - Y}{g_b^{\frac{1}{2}}}\right] = m\left[\frac{Y_s - Y}{g_b^{\frac{1}{2}}}\right]. \tag{9}$$

This introduces a new unknown, Y, which is the ratio of the equilibrium partial pressure at T_b to the total pressure. It has here been assumed that mass fractions are identical with mole fractions, requiring comparable molecular weights between species. Assuming the latent heat is constant with temperature, a simplified relation is [8]

$$Y = Y_{F_0} \exp\left[\varepsilon_v(1 - g_L^\circ/g_b)\right]. \tag{10}$$

Only as $m \to \infty$ can an equilibrium interface be assumed. There are, however, several practical combustion regimes where m is 0[1]. This will occur in a low pressure, high velocity environment with sufficiently small drop size and a fuel with a low α. The first three requirements are satisfied if the mean free path becomes sufficiently large compared with the drop size; m/α is a measure of the validity of the continuum flow assumption. For the analysis to be valid $m/\alpha \gg 1$ must be assumed. However, m can still be 0(1) if α is low which can occur if the fuel has special molecular properties or is contaminated in some sense [6].

Equations (1) subject to equations (6)–(10) represent the problem to be solved. The new elements in this calculation are in equations (6) and (9) which contain liquid phase heat transfer and finite evaporation kinetics. The approach to the solution could consist of an algebraic one; it is well known that solutions exist in the

literature to the first two of equations (1) subject to the temperature boundary conditions and equations (7). These solutions, as in [9], would yield g' as functions of g_b and f_0 to which a curve fit could be applied; equation (6) then yields a relation between g_b and f_0. The mass fraction equation of equations (1) subject to the first of equations (1) imply a linear relation between g and Y_F. Equations (6) and the last of equations (8) then imply an algebraic relation between Y_s, f_0 and g_b. Equations (9) and (10) then provide sufficient equations in the unknowns g_b, f_0, Y_s and Y. This procedure was not adopted because there are insufficient numerical integrations of equations (1) in the literature for a Prandtl number of unity which cover the values of f_0 and g_b of interest in this paper. To carry out the numerical integrations in this work was deemed costly considering the number of calculations to be made. Consequently, the approach taken was to apply the method of weighted residuals to the problem as outlined in [10].

The velocity profile is approximated by

$$f' = (a_1\eta + a_3\eta^2 - 1)\,e^{-a_2\eta} + 1$$

with the a's as constants to be determined. This satisfies equation (7) but with f_0 undetermined. The temperature profile is chosen as

$$g = [b_1\eta + b_3\eta^2 + (g_b - 1)]\,e^{-b_2\eta} + 1$$

and the fuel mass fraction is chosen as

$$Y_F = (c_1\eta + Y_s)\,e^{-c_2\eta}.$$

These functional forms are placed into equations (1), weighted by a function, and integrated from 0 to ∞; this yields algebraic equations in the unknown constants. Enough weighting functions are chosen to yield as many algebraic equations as there are unknowns. The weighting functions for the momentum equation have been chosen as

$$e^{-a_2\eta},\ \eta e^{-a_2\eta},\ \eta^2 e^{-2\eta},$$

those for the energy equation

$$e^{-b_2\eta},\ \eta e^{-b_2\eta},\ \eta^2 e^{-b_2\eta},$$

and those for the mass fraction equation

$$e^{-c_2\eta},\ \text{and}\ \eta e^{-c_2\eta}.$$

The resulting nonlinear, algebraic equations will not be presented here since they are quite lengthy and since one purpose here is to perform calculations once and for all. Regardless, eight algebraic equations are produced in the twelve unknowns a_1, a_2, a_3, b_1, b_2, b_3, c_1, c_2, f_0, Y_s, Y and g_b. The four remaining algebraic equations come from equations (6), the diffusion relation of equations (8), and equations (9) and (10) into which the approximating functions are directly placed. These twelve equations are solved by iteration. Usually four iterations are all that are required for acceptable accuracy since initial estimates of the unknowns are relatively simple to make from physical knowledge of the system.

The procedure above is closely related to a truncated expansion of the solution in terms of Laguerre functions 11 which form a complete, orthogonal set in the interval 0, ∞. However, the appearance of the constants a_2, b_2 and c_2 as well as the use of simple powers of η as multipliers negates the viewpoint of a Laguerre function expansion. Completeness of the set of functions is not claimed; however, without proof, it is conjectured that the more terms retained in the expansion the more accurate should be the results. The reason for including the scale factors a_2, b_2 and c_2 is to make a more rapid convergence to the answer, because the exponential term dominates the distance scale of decay. It is imperative with an approximate technique of this type that an estimate be given of the accuracy of the method. Two ways exist to perform the demonstration that reasonable results are obtained. The first consists of demonstration that taking more and more terms of the expansion gives numerical convergence. The second, and the one adopted here, is to compare the results with an exact solution, since, as has been mentioned, some solutions for g' as a function of g_L and f_0 exist.

Accordingly, from the numerical results Fig. 2 can be drawn expressing the gas phase interface

heat transfer as a function of the wall blowing rate and interface temperature. The circled points are exact calculations taken from [9]. Since the calculations in [9] are for a Prandtl

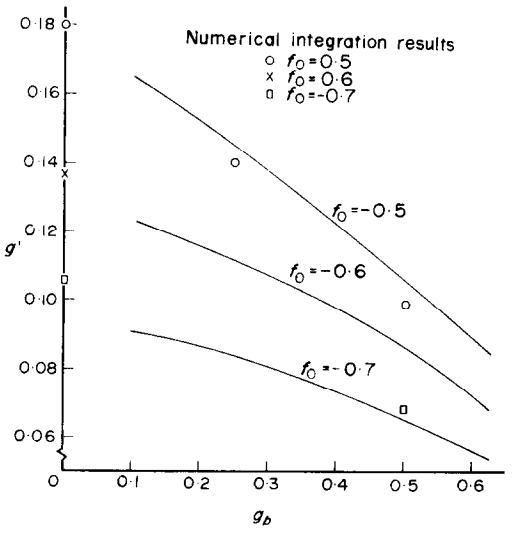

FIG. 2. Comparison of approximate method with adjusted numerical integrations.

number of 0·7, these calculated points have been adjusted by the factor

$$\frac{g'\,(\text{Prandtl No.} = 1)}{g'\,(\text{Prandtl No.} = 0{\cdot}7)} = 1{\cdot}1533$$

from the work of Sibulkin [12]. It is seen that the agreement of the present method and exact numerical integrations (adjusted) is quite good; generally 10 per cent accuracy is achieved. This error is well within the magnitude of effects to be elucidated in this paper and within errors in combustion analysis in general.

Entire droplet

As the quantity B drops it may be seen from equation (6) and may be verified later that the portion of heat transfer going toward providing the latent heat increases relative to that going toward liquid heat transfer. The experiments usually quoted in providing the relation*

$$\frac{\dot{m}\,(\text{convection})}{\dot{m}\,(\text{no convection})} = 1 + 0{\cdot}3\,Re^{\frac{1}{2}} \qquad (11)$$

are based upon low B configurations, as in [13] or [14]. The Reynolds number in equation (11) is based upon the droplet diameter and free stream properties. An accepted method [15] of computing $\dot{m}$ (no convection) is $4\pi\mu_\delta a \ln[1 + B(1 - g_b)]$. This formula is, however, not correct in cases where strong heat transfer to the liquid is occurring. Equation (11) is undoubtedly incorrect in fine detail near $Re = 0$, as expressed in [16], but it is of practical use. The present theory is restricted to $Re \gg 1$ so for the moment consider the high Re form of equation (11) by dropping the 1. In view of the foregoing remarks, if calculations of the present paper are taken where $g_b = g_{L_0}$ (no heat transfer to the liquid phase), the results should give the ratio of total droplet vaporization rate to the stagnation point rate through the use of equations (11) and (5). That is, taking equation (5) and assuming $(du/dx)_0 \propto (u_\infty/a)$ along the result $\bar{m}$ (no convection) $= 0{\cdot}3\ Re^{\frac{1}{2}}(\mu_\delta/a)\ \ln[1 + B(1 - g_b)]$ and dividing the two it is found that the ratio

$$\frac{-f_0}{\ln[1 + B(1 - g_b)]}$$

should be constant. Table 1 gives the comparison which shows that well within

Table 1

g_b	B	$-f_0$	$-f_0/\ln[1 + B(1 - g_b)]$
0·8	3·15	0·235	0·48
0·6	1·6	0·235	0·47
0·4	1·1	0·233	0·46

$m = 100$, $\varepsilon_v = 13{\cdot}0$, $Y_{F_0} = 0{\cdot}4$, $g_b = g_{L_0}$

the accuracy of the analysis the correspondence holds between the present boundary-layer theory and the empirical correction to a spherically symmetric theory. Using the average number of

* A weak dependence on the Prandtl and Schmidt numbers is omitted here.

this ratio it is determined

$$\frac{\bar{m}}{\bar{m}_{\text{Stag. pt.}}} = 0{\cdot}52$$

or the vaporization rate per unit area averaged over the entire droplet is 52 per cent of the stagnation point value. The suggestion naturally follows, therefore, that the present results may be used to compute total droplet vaporization rates. First, it follows that

$$\dot{m} = 4\pi a^2 \bar{m} = 4\pi a^2 (0{\cdot}52)\, \bar{m}_{\text{Stag. pb.}}$$

(11) to broaden the range of applicability of the results. There follows

$$\dot{m} = (1 + 0{\cdot}3\, Re^{\frac{1}{2}})(53)\, \mu_\delta a(-f_0). \qquad (12)$$

Equation (12) is offered as a formula for computation of droplet vaporization rates regardless of Reynolds number where f_0 is given below as as a function of several parameters.

It is to be emphasized that equation (12 has been constructed to agree with the present body of experimental results. It recovers the mass transport results of [13] and [14]. The formula

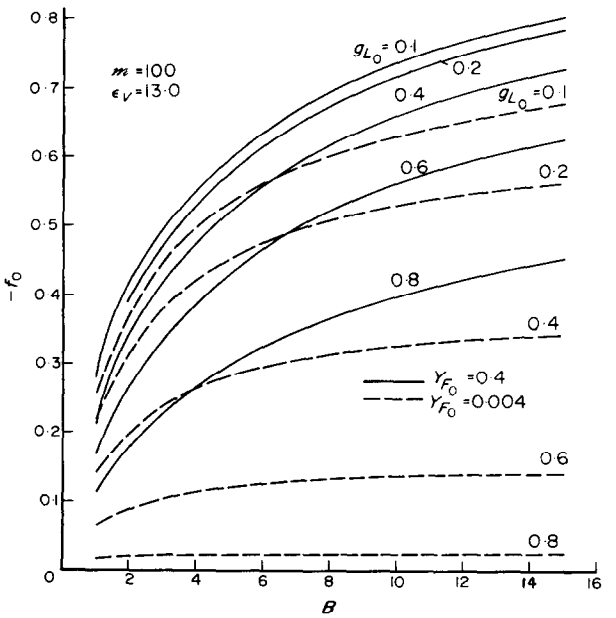

FIG. 3. Vaporization rate vs. B for selected parameters.

Assuming $(du/dx)_0 = \frac{3}{2}(u_\infty/a)$, the low speed inviscid value of the velocity gradient, equation (5) yields

$$\bar{m}_{\text{Stag. pt.}} = 6^{\frac{1}{2}} Re^{\frac{1}{2}} \frac{\mu_\delta}{a}(-f_0) = 0{\cdot}3\, Re^{\frac{1}{2}} \left(\frac{6^{\frac{1}{2}}}{0{\cdot}3}\right) \times \frac{\mu_\delta}{a}(-f_0)$$

where Re is based on the same properties as in equation (11). A suggestion then is to replace the factor $0{\cdot}3\, Re^{\frac{1}{2}}$ by $1 + 0{\cdot}3\, Re^{\frac{1}{2}}$ as in equation

contains the well known high Re form of the Nusselt number [17], being proportional to $Re^{\frac{1}{2}}$. Of course, there is presently no experimental support for equation (12) for high B configurations. Consequently the applicability of equation (12) must be regarded as a conjecture, since it appears correct in limiting cases but has incomplete supporting evidence for general applicability.

STAGNATION POINT RESULTS

For fixed $\dot{m}$, ε_v, Y_{F_0} Figs. 3–5 show the

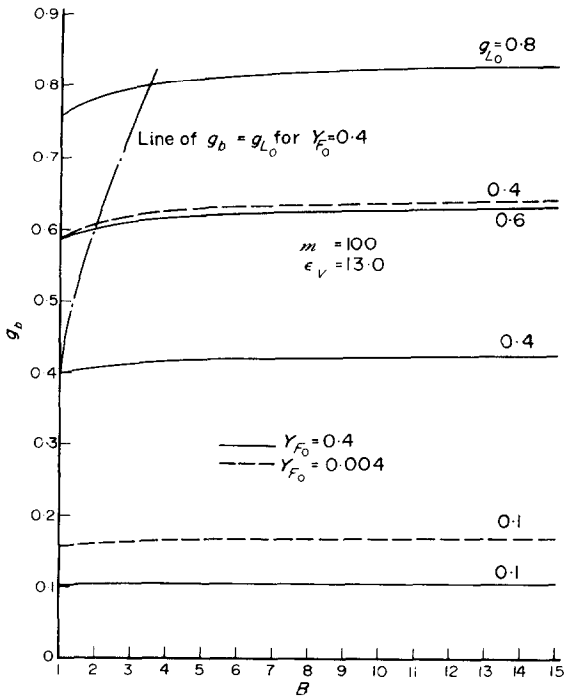

FIG. 4. Surface temperature vs. B for selected parameters.

vaporization rate (f_0), surface temperature (g_b) and droplet vapor mass fraction at the interface (Y_s) as a function of B with g_{L_0} a parameter. By a highly volatile fuel it is meant in this paper that the vapor pressure at the initial temperature is high. Since mass transfer in significant amounts requires high Y_s, a fuel with high Y_{F_0} means that little interface heat-up (or temperature change in any direction) is required. Consequently, for any given g_{L_0} it is seen on Fig. 3 that mass transfer at any given B is significantly higher for a more volatile fuel. Furthermore, comparing $1/B$ with $g_b - g_{L_0}$ as in equation (6) it is seen that a much lower fraction of heat transfer goes toward liquid heat transfer for the more volatile fuel. Of greater significance is the general fact that the liquid heat transfer can be substantially greater than that going toward providing the latent heat as shown by the example of Table 2.

Table 2

Y_{F_0}	$1/B$	$g_b - g_{L_0}$	f_0	Ratio of liquid phase heat transfer to latent heat provision $(g_b - g_{L_0}) \times B$
0·004	0·1	0·24	0·327	2·4
0·4	0·1	0·024	0·656	0·24

$m = 100$, $\epsilon_v = 13{\cdot}0$, $B = 10$, $g_{L_0} = 0{\cdot}4$

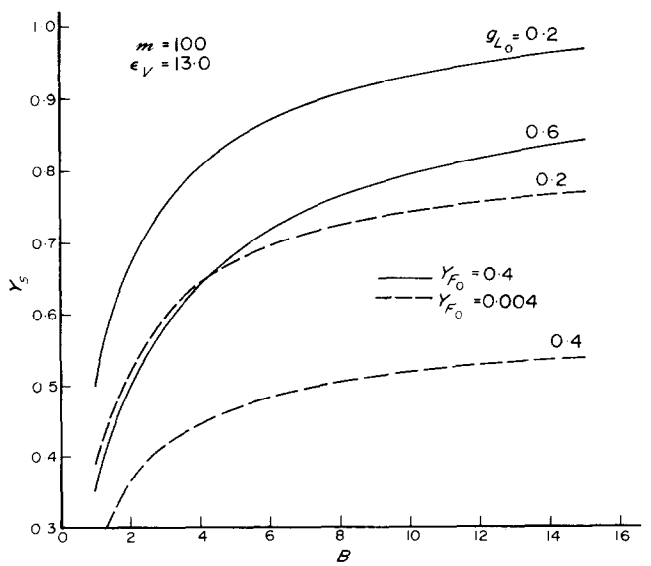

FIG. 5. Surface fuel mass fraction vs. B for selected parameters.

Consequently, the fact that a wet-bulb condition is not attained under the present assumptions cuts drastically into the computed vaporization rate for non-volatile fuels and requires a significant correction for even volatile fuels. The assumption of wet-bulb attainment can easily lead to errors in the computed vaporization rate of the order of a factor of 2.

Other facts shown by Figs. 3–5 are less subtle. As B increases for fixed g_{L_0}, f_0, g_b and Y_s increase. This is the consequence of a lower latent heat. The latent heat also enters into ε_v but this will be shown to have a minor effect on the primary quantities of interest. As g_{L_0} rises for fixed B, $|f_0|$ falls. It should be emphasized that this is not the effect of raising T_{L_0} because Y_{F_0} and m have been held fixed. Additionally it is not the effect of lowering T_δ because B is fixed. Perhaps the easiest way to visualize the g_{L_0} change is that T_b is raised as the fuel is changed to maintain Y_{F_0} at a fixed value. That is, a higher g_{L_0} corresponds to a less volatile fuel, and, since the heat-transfer potential from T_δ to T_b decreases, $|f_0|$ decreases. It should be

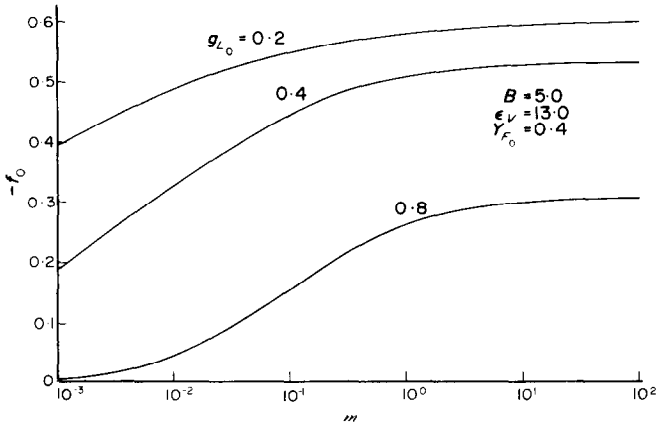

FIG. 6. Vaporization rate vs. kinetics parameter.

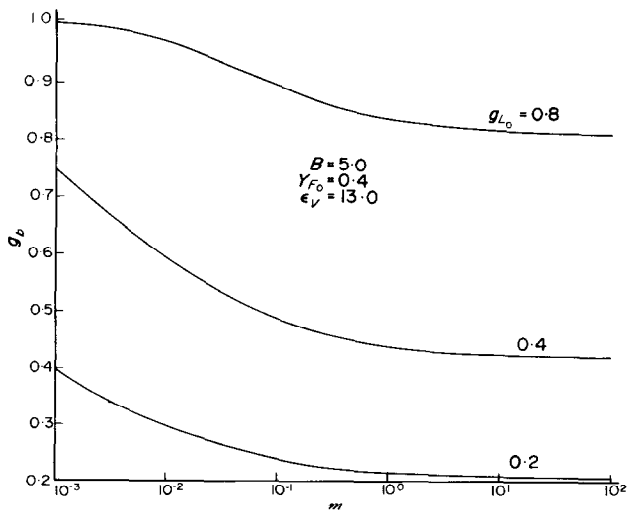

FIG. 7. Surface temperature vs. kinetics parameter.

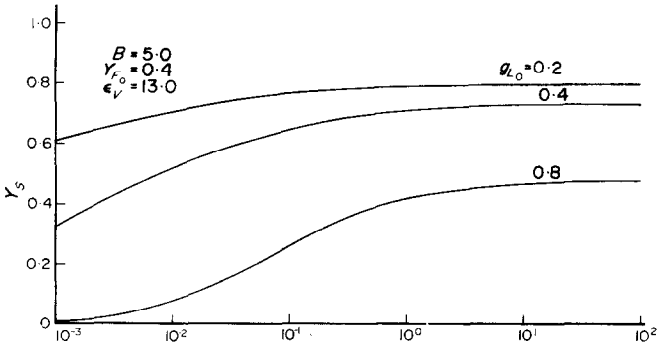

FIG. 8. Surface fuel mass fraction vs. kinetics parameter.

noted in Fig. 4 that at sufficient low B cooling of the interface, rather than heating, occurs (mass transfer cooling). g_b falls below g_{L_0}.

Figures 6–8 show the effects of finite vaporization kinetics. In most combustion situations in the aerospace field typical values of m are from 0·1 to 1000. It is seen that a reasonable reduction of vaporization rate can occur at the lower end of the m range and the reduction is more pronounced the larger the value of g_{L_0}. The effect of slow vaporization kinetics is to force the surface temperature higher for a given mass-transfer rate; since a higher surface temperature implies more heat transfer to the liquid phase, there is in turn a reduction of heat transfer to provide the latent heat. Consequently, the vaporization rate decreases. Presently, the greatest uncertainty in m is α which depends heavily upon the liquid phase structure and possible surface contaminants.

Figure 9 shows the effect of ε_v on the vaporization rate. ε_v measures the slope of the vapor pressure vs liquid temperature curve. All other factors equal a high ε_v means the surface temperature change from g_{L_0} must be smaller to accomplish a given outward mass transfer rate. Hence, less heat transfer to the liquid is required and the vaporization rate increases with ε_v, all other factors held constant. This is, however, a weak effect as is seen in Fig. 9.

The separate effect of Y_{F_0} is shown in Fig. 10. The nearly linear behaviour of f_0 vs. ln Y_{F_0} will be shown below to greatly aid in the use of these curves for computing the vaporization rate of any given configuration.

Within the previously stated accuracy of the analysis sufficient calculations have been presented to cover a wide range of conditions. The primary parameters which have a strong effect on f_0 are B, g_{L_0} and Y_{F_0}. Although the direct effect of Y_{F_0} is small, in practice this parameter

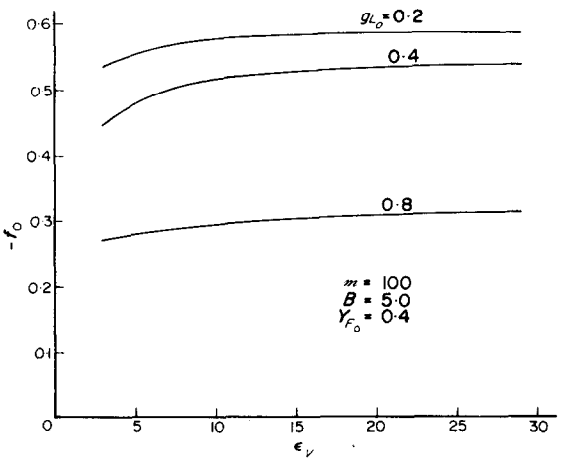

FIG. 9. Vaporization rate dependence on ε_v.

varies over a wide range. It is therefore suggested that any configuration can be computed to reasonable accuracy by the following procedure:

1. From Fig. 3 obtain f_0 for $Y_{F_0} = 0{\cdot}4$ and 0·004 for the given values of g_{L_0} and B.

2. With the known Y_{F_0} compute a corrected f_0 by linear interpolation using the logarithm of Y_{F_0}.
3. Make the minor m and ε_v corrections using linear interpolation and Figs. 6 and 9.

An example of this procedure is shown for a 50–50 mixture of UDMH–N_2H_4 using property data from [18]. The conditions chosen are $T_{L_0} = 500°R$ $p = 300$ psia, $T_\delta = 5000°R$ so that

$$g_{L_0} = 0{\cdot}105 \quad Y_{F_0} = 0{\cdot}00308$$
$$B = 8{\cdot}13 \quad \varepsilon_v = 9{\cdot}98$$
$$m = 55{\cdot}6 \quad \alpha = 1 \text{ (assumed)}.$$

Exact calculations by the procedure of this paper yield $f_0 = -0{\cdot}539$. From Fig. 3

$B = 8{\cdot}13$, $g_{L_0} = 0{\cdot}105$, $m = 100$, $Y_{F_0} = 0{\cdot}4 \rightarrow f_0 = -0{\cdot}695$

$B = 8{\cdot}13$, $g_{L_0} = 0{\cdot}105$, $m = 100$, $Y_{F_0} = 0{\cdot}004 \rightarrow f_0 = -0{\cdot}595$.

Linear extrapolation with log Y_{F_0} then yields

$$f_0 = -0{\cdot}537$$

which may be compared with the exact result. Corrections with respect to m and ε_v could also be made, but they are minor. It is seen that the result is well within the accuracy of the analysis. Hence, the results presented herein offer a method of rapidly estimating the vaporization rate for a wide variety of practical combustion situations.

DISCUSSION AND CONCLUSIONS

Calculations have been presented for the case of stagnation point vaporization rates in a high

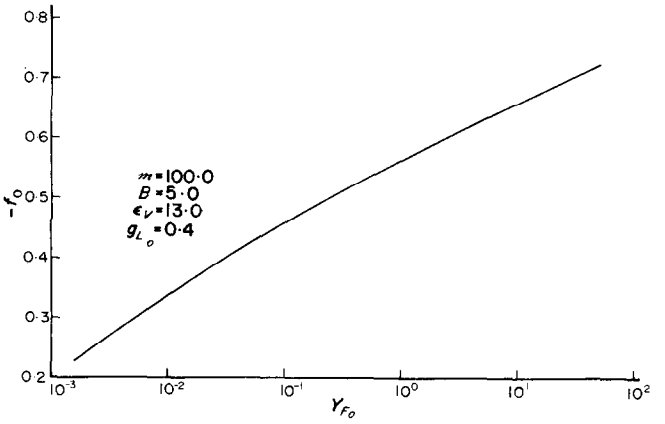

FIG. 10. Vaporization rate dependence on volatility.

Reynolds number flow when the liquid–gas interface is out of equilibrium and for the case of no internal circulation in the liquid. A method which agrees with the present body of experimental data has been developed for the computation of entire droplet vaporization rates from the known stagnation point rate. Sufficient calculations have been presented to make engineering estimates of vaporization rates for a wide variety of high temperature vaporization situations.

Because of the heat transfer into the liquid when a thermal wave exists vaporization rates can be substantially lower than those computed from conventional formulas which assume the attainment of a wet bulb temperature. The assumption of no internal circulation appears justifiable on the basis of current knowledge but there clearly is a need for diagnostic experiments or at least theoretical work in both the high and low Reynolds number regimes to clarify this issue. The present theoretical results

should also be viewed as upper limits to the vaporization rate under the no internal circulation assumption, because the thermal wave development transient in any real situation requires of the order of a droplet lifetime [3]. During this transient the thermal wave is thinner than its fully developed form, and consequently the amount of heat transfer into the liquid is greater than it would be if a steady state had been achieved.

ACKNOWLEDGEMENT

The author would like to thank Mr. W. K. Juneja for performing the weighted residuals calculations.

REFERENCES

1. R. J. PRIEM and M. F. HEIDMANN. Propellant vaporization as a design criterion for rocket engine combustion chambers, NASA TR R-67 (1960).
2. H. SCHLICHTING. *Boundary Layer Theory*. p. 188. McGraw-Hill, New York (1960).
3. W. C. STRAHLE, A transient problem on the evaporation of a reactive fuel. *Combustion Science and Technology* **1**, 25 (1969).
4. J. G. SOTTER, Nonsteady evaporation of liquid propellant drops: The Grossman model. Jet Propulsion Laboratory Technical Report 32–1061 (1968).
5. H. W. EMMONS, The film combustion of a liquid fuel. *Z. Angew. Math. Mech.* **36**, 60 (1956).
6. S. S. PENNER. On the kinetics of evaporation. *J. Phys. Chem.* **56**, 475 (1952).
7. W. C. STRAHLE. New considerations on causes for combustion instability in liquid propellant rockets. *Combustion Science and Technology* **2**, 29 (1970).
8. S. GLASSTONE. *Physical Chemistry* p. 452. Van Nostrand, New York (1959).
9. E. RESHOTKO and C. B. COHEN. Heat transfer at the forward stagnation point of blunt bodies. NACA TN 3513 (1955).
10. W. F. AMES. *Nonlinear Partial Differential Equations in Engineering*. p. 243. Academic Press, New York (1965).
11. I. N. SNEDDON. *Special Functions of Mathematical Physics and Chemistry*. p. 148. Interscience, New York (1956).
12. M. SIBULKIN, Heat transfer near the forward stagnation point of a body of revolution. *J. Aero. Sci.* **19**, 570 (1952).
13. W. F. RANZ and W. R. MARSHALL. JR., Evaporation from drops, pt. I. *Engng. Prog.* **48**, 141 (1952).
14. N. A. FUCHS. *Evaporation and Droplet Growth in Gaseous Media*. Pergamon, Oxford (1959).
15. F. A. WILLIAMS. *Combustion Theory*. p. 54. Addison-Wesley, Reading, Mass (1965).
16. A. J. EGGERS, JR., C. F. HANSEN and B. E. CUNNINGHAM. Stagnation point heat transfer to blunt shapes in hypersonic flight, including effects of yaw. NACA TN 4229 (1958).
17. F. E. FENDELL, D. E. COATS and E. B. SMITH. Compressible slow viscous flow past a vaporizing droplet. *AIAA Jl* **6**, 1953 (1968).
18. ANON., Performance and properties of liquid propellants: Revision A. Aerojet General Corporation (1961).

EVAPORATION DE GOUTTES PAR CONVECTION FORCEE AVEC UNE CINETIQUE DE VAPORISATION FINIE ET UN TRANSFERT THERMIQUE

Résumé—Des calculs au point d'arrêt, comprenant les effets de transfert thermique dans la phase liquide et des cinétiques de flux d'évaporation fini sont présentés pour le cas d'un écoulement à grand nombre de Reynolds autour d'une goutte en évaporation. On développe une relation pour calculer le taux d'évaporation globale de la goutte à partir des résultats obtenus pour le point d'arrêt. Une extension numérique est relative au cas des processus de vaporisation rapide à température élevée comme cela se rencontre dans les moteurs de véhicules volants et on présente des calculs qui constituent des approches de cas réels quelconques.

TROPFENVERDAMPFUNG BEI ERZWUNGENER KONVEKTION MIT ENDLICHER VERDAMPFUNGSWÄRME UND FLÜSSIGKEITS-WÄRMEÜBERGANG

Zusammenfassung—Staupunkt-Rechnungen, mit Berücksichtigung des Einflusses des Wärmeübergangs im Flüssigkeitsgebiet und endlicher Verdampfungswärme, werden für Umströmung eines verdampfenden Tropfens bei hohen Reynolds-Zahlen ausgeführt. Es wurde eine Beziehung entwickelt zur Berechnung der gesamten Tropfenverdampfung aufgrund der Staupunkt-Rechnung. Grosser Wert wurde auf die Berechnung von schnellen Verdampfungsprozessen bei hohen Temperaturen gelegt, wie sie in Flugzeugtriebwerken auftreten; es wurden genügend numerische Ergebnisse vorgelegt, um Abschätzungen für jeden möglichen Fall zu machen.

КИНЕТИКА ИСПАРЕНИЯ КАПЕЛЬ С КОНЕЧНОЙ СКОРОСТЬЮ И ТЕПЛООБМЕН В ЖИДКОСТИ ПРИ СВОБОДНОЙ КОНВЕКЦИИ

Аннотация—Представлены расчеты для критической точки при обтекании испаряющейся капли при больших числах Рейнольдса. При этом учитывается влияние теплообмена и кинетики испарения с конечной скоростью. Получено обощенное уравнение для расчета интегральной скорости испарения капли. Численные расчеты проводятся для высокотемпературных процессов с большой скоростью испарения, как, например, в авиационных двигателях. Также представлены расчеты, применимые для любого данного случая.